

Volume III: Calorimeter

We propose a hodoscopic scintillation crystal calorimeter with PIN photodiode readout to meet the scientific requirements for the GLAST mission within the specified mass and power budgets. Crystal scintillators are a mature technology with an extensive history of use in space, allowing us to focus the calorimeter development efforts on detailed design issues and technology challenges such as (1) minimization of the effects of the mechanical design on science performance, (2) optimization of calorimeter-only imaging, and (3) a low-power, large dynamic-range readout system. The proposed program provides for the fabrication of a prototype calorimeter which demonstrates technology readiness level 6 for all critical calorimeter technologies.

III.1 Overview of the GLAST Calorimeter

The calorimeter in a pair-conversion gamma-ray telescope is critical in determining the energy range, energy resolution, and background-rejection capability of the telescope. A calorimeter is typically constructed of a high Z, active detector material, although various passive/active sampling techniques can be employed.

The primary tasks of the GLAST calorimeter are to provide an accurate measure of the energy of the shower resulting from pair conversion of incident gamma rays in the tracker, and to assist with cosmic-ray background rejection through correlation of tracks in the precision silicon tracker with the position of energy deposition in the calorimeter.

To perform these tasks, the calorimeter should have the following properties.

- The calorimeter must have adequate depth to contain most of the energy of the gamma-ray showers. Generally this means that shower maximum must be within the detector.
- The calorimeter must contain a sufficiently high fraction of active detector materials that the total energy measurement is not dominated by “sampling” statistics.
- The energy resolution must be adequate to measure spectral breaks already observed or theoretically predicted from celestial sources.
- The calorimeter must provide some crude imaging capability or physical segmentation to allow the correlation of events in the tracker with energy depositions in the calorimeter.
- The calorimeter should be stable against aging and environmental changes, e.g. temperature and

magnetic field variations on orbit. It should be easy to calibrate.

We propose a segmented thallium-doped cesium iodide, CsI(Tl), scintillation crystal calorimeter for the GLAST instrument. This technology can meet or exceed all of the identified requirements for the GLAST mission. To achieve the required energy coverage and resolution, the calorimeter is 10 radiation lengths ($10 X_0$) deep. To assist in track correlation for background rejection, the calorimeter is segmented into discrete detector elements.

The segmented CsI calorimeter that we propose provides a valuable imaging capability for high-energy ($E > 1$ GeV) photons that convert in the calorimeter rather than in the tracker. ***This doubles the effective area and significantly broadens the field of view of the instrument at high energies. We emphasize that this calorimeter-only imaging capability provides an enhancement to GLAST beyond those goals specified***



Figure III-1. Calorimeter compression cell design. For clarity, one panel of compression bars is not shown. The figure shows a partial stack of CsI crystals to emphasize the stacking concept.

in Table I-1. This capability is particularly useful for pulsar timing and pulse-phase spectroscopy, and for spectroscopic and time-variability studies of gamma-ray bursts (GRBs) and active galactic nuclei (AGN), where it is important to collect as many source photons as possible. In addition, segmentation of the calorimeter gives GLAST the ability to determine the shower energy-loss profile in the calorimeter, which improves the detector absolute calibration and energy resolution by allowing for correction of shower leakage fluctuations.

The CsI crystal array is fully compatible with the modular design of the proposed full GLAST system, with each of the 25 “tower” modules containing anti-coincidence, tracker/converter, and calorimeter subsystems functioning together (and testable as an autonomous system).

The CsI(Tl) scintillation crystal has a well-established history for calorimetry in a number of ground-based and space-based experiments. It provides excellent intrinsic energy resolution at modest cost, provides a fairly fast signal, and is reasonably radiation hard. CsI(Tl) is also a much more rugged material than NaI(Tl) and is comparatively not hygroscopic, greatly reducing the cost and complexity of construction and handling.

The scintillation crystals are read out with PIN photodiodes. The spectral response of diodes is well matched with the scintillation spectrum of CsI(Tl), which provides for a large primary signal (~10,000 photoelectrons generated per MeV deposited), with correspondingly small statistical fluctuations and thereby high intrinsic spectral resolution. Photodiodes have relatively low operating voltages (~50 V), which simplifies their use in space relative to photomultiplier tubes. They are extremely rugged and have small physical dimensions, which minimize the amount of passive material and empty volume in the calorimeter.

The basic technologies for the GLAST calorimeter have a proven history of success in space applications. However, we must still resolve a number of technical challenges to achieve the science performance in the detailed design, namely:

- minimization of passive material in the calorimeter, which affects energy resolution;
- minimization of angular uncertainties in the reconstructed track directions for calorimeter-only events;

- provision of a sufficiently low-power calorimeter readout that covers the extremely broad dynamic range of energy losses (about 3×10^5 for the proposed design).

The Proposed Calorimeter Configuration III.2

The proposed modular calorimeter is built on a hodoscopic arrangement of CsI(Tl) scintillation crystals with PIN photodiode readouts. Each GLAST tower contains 80 crystals of size 3.0 cm \times 2.3 cm \times 31 cm. The crystals are individually wrapped for optical isolation, and are arranged horizontally in 8 layers of 10 crystals each. Each layer is rotated 90° with respect to its neighbors, forming an x - y array. (See Figure III-2, for example.) PIN photodiodes mounted on both ends of a crystal measure the scintillation light from an energy deposition in the crystal that is transmitted to each end. The difference in light levels provides a determination of the position of the energy deposition along the CsI crystal. The position resolution of this imaging method ranges from a few millimeters for low energy depositions (~10 MeV) to a fraction of a millimeter for large energy depositions (>1 GeV), as demonstrated in Section III.4. ***Thus the hodoscopic CsI array, with its simple PIN diode readout, gives positioning performance comparable to that of scintillating fiber calorimeters and provides better energy resolution, particularly at low energies.***

The hodoscopic CsI calorimeter has been designed to meet or exceed the specifications for the GLAST mission reflected in Table 2 of the NRA. Table III-1 summarizes the GLAST requirements relevant to the calorimeter. To achieve the large required dynamic

Parameter	Requirement
Energy Range	0.02 - 300 GeV
Energy Resolution	25% (10 MeV - 300 GeV)
Field of View (FWHM)	>2 sr
Effective Area	>7000 cm ² (>1 GeV) >3500 cm ² at 50 GeV
Dead Time	<10% at 5 kHz
Instrument Lifetime	5 yrs, with no more than 20% degradation.

Table III-1. GLAST Measurement Requirements Relevant to the Calorimeter

range of the readout, four photodiodes will be used on each crystal, two on each end, attached to preamplifiers with differing gains.

The size of the CsI crystals has been chosen as a compromise between electronic channel count and desired segmentation within the calorimeter. The indicated size is comparable to the CsI radiation length (1.86 cm) and Moliere radius (3.8 cm) for electromagnetic showers. The size of the crystals is not the dominant factor in determining the imaging capabilities of the calorimeter because most of the positional information is provided by the light-difference measurement; nevertheless finer sampling provided by smaller crystals (1.5 to 2 cm) in at least the first few layers of the calorimeter would provide better angular resolution for calorimeter-only gamma-ray events. Simulations of the imaging capability of the calorimeter are being performed to further optimize this segmentation.

Figure III-1 shows the compression frame that holds the crystals in place against Delta II launch loads. Signals from the PIN diodes pass through the frame on flex circuits to the analog front-end electronics, which are mounted on narrow printed circuit boards fastened between the vertical mechanical members of the frame. The entire calorimeter compression cell will be surrounded by an electromagnetic shield and an optical shield (not shown in Figure III-1). Signals from the front-end electronics will travel down the boards and connect to a data acquisition controller board located under the base of the calorimeter. That controller will interface with the GLAST data acquisition system (DAQ) for each tower.

III.3 Projected Performance of the Calorimeter

From extensive Monte Carlo simulations of the baseline calorimeter, along with laboratory tests and accelerator measurements of prototype hardware, we can project the science performance of the proposed CsI hodoscopic calorimeter for GLAST. Preliminary electronic and mechanical designs allow us to estimate the mass and power required to implement this calorimeter in space.

1. Energy Range. Our laboratory tests demonstrate that the lowest measurable energy using the technology proposed for this calorimeter is ~ 600 keV in a single crystal. The low energy limit of the combined instrument is therefore set by the low energy limit on pair conversions in the tracker, not the calorimeter. The highest energy gamma ray reliably measured with this



Figure III-2. Partially assembled hodoscopic 6x8 CsI crystal array prior to beam test.

calorimeter is determined by the highest energy electromagnetic shower whose maximum of energy deposition can be identified within the calorimeter. On axis, for a $10X_0$ calorimeter, that energy is ~ 300 GeV. Off axis, this maximum increases and showers with energies above 1 TeV should be measurable with an energy resolution within the specifications.

2. Energy Resolution. At low energies, the GLAST energy resolution will be limited by the uncertainty of the energy loss in the tracker, because the intrinsic calorimeter energy resolution is measured to be less than 8% below 3 MeV. Quantization error (~ 100 keV for the lowest energy range) in the flight electronics is negligible, even at threshold. Nuclear activation of the CsI crystals is a minor contributor to the energy resolution near threshold. It causes a non-negligible fraction of good events to be accidentally coincident with a background decay, adding an unpredictable amount of energy to the measurement. However, we calculate this to contribute no more than 1 MeV to the energy resolution at all energies. For events with energies of hundreds of MeV, the main contributor to the energy resolution will be the energy loss in passive materials in the tracker, calorimeter, and between towers. This is one of the reasons to minimize passive material. Monte Carlo simulations show that this loss is less than 10 MeV in the worst-case geometry. At energies above 1 GeV, the main contributor to the energy uncertainty is the energy leakage out of the bottom or sides of the calorimeter. The next section will show how this effect can be corrected to better than 10%.

Energy (GeV)	Hodo Cal	HodoCal Stretched	HodoCal w/ Vertex	Stretched w/ Vertex
1	6°	3°	2.0°	0.6°
10	2°	1°	0.6°	0.2°

Table III-2. Angular resolution of various hodoscopic calorimeter designs. The vertex detector is a Si strip module inserted in the calorimeter. The Stretched calorimeter adds a 20-cm gap within the calorimeter to increase the lever arm.

The energy resolution of the proposed calorimeter is therefore better than the 25% goal stated in the NRA.

3. Imaging Capability. The hodoscopic segmentation of the calorimeter makes the calorimeter alone a gamma ray imaging device. *This is a significant enhancement over the goals of the baseline calorimeter since more than half of the incoming photons do not interact in the baseline tracker.* In section III.4, we will show that the calorimeter crystals can position events with an accuracy ranging from a few millimeters to a fraction of a millimeter, depending on the energy deposited. Calorimeter-only imaging will double the effective area at high energies, and the high-precision positions and long lever arm can also be used to more accurately image the high-energy events that do convert in the tracker.

4. Angular Resolution. The angular resolution achievable with the calorimeter-only events depends on the detailed geometry of the calorimeter. The imaging capabilities of the calorimeter can be improved by extending the distance, or lever arm, over which electromagnetic shower positions are measured. This could be achieved by adding a gap between some or all layers of the calorimeter. We plan to investigate this possibility with Monte Carlo simulations and to study the degradation in energy resolution expected from extra support structures required by this modification.

Significant improvements in calorimeter imaging can be achieved by inserting an x-y pair of Si trackers a small distance into the calorimeter to position the vertex of the shower, while the deeper layers of the calorimeter measure the direction of the shower. These improvements come at the cost of additional mechanical and electrical complexity; however, we will continue to investigate this possibility with simulations.

Table III-2 compares the performance of the proposed hodoscopic calorimeter with that of a calorimeter of identical geometry with a Si vertex detector inserted

and that of a “stretched calorimeter” with vertex detection and a 20-cm gap after the first $3X_0$.

5. Calibration. It is important to have an absolute energy calibration of the GLAST calorimeter as it operates on orbit. Radionuclide dopants or alpha flashers can provide several MeV-equivalent energy loss and could be used to calibrate the highest gain scale (i.e. the lowest energy range). Similarly an actively controlled LED flasher system could provide a programmable energy point, although the mechanical complexity of delivering an LED pulse to each crystal could be high, and there is some concern about the stability of the optical and active feedback mechanism over time.

The high flux of relativistic medium and heavy galactic cosmic rays (GCRs) provides an alternative on-orbit calibrator. Minimum-ionizing C and Fe, at normal incidence, deposit typically ~ 800 MeV and ~ 15 GeV in each CsI bar, and the rate of these GCRs, ~ 50 Hz traversing the calorimeter through its upper and lower surfaces, is adequately high to allow calibrations to accumulate in a reasonable time, but not so high that the downlink data volume is stressed.

The ACD would be configured to veto events that deposit some fraction of a minimum ionizing particle (MIP) to several MIPS, but to flag events that deposit more than several MIPS. For each valid particle, the full GLAST array would be triggered. On the ground, trajectories would be determined from the tracker. After correcting for the derived pathlength in each CsI bar, the dE/dx would be accumulated and used for calibration.

From the CREME96 cosmic-ray propagation software and the known nuclear-interaction cross sections, we estimate that there would be ~ 900 non-interacting CNO-group and ~ 50 non-interacting Fe-group nuclei in each CsI bar every day, which are more than adequate to achieve an energy calibration with a statistical precision of $\sim 1\%$ each day.

6. Power and Mass Budget. Using the design of the prototype ASIC already under development, we estimate that the power requirement for the calorimeter is approximately 5 W per tower (see Table III-3). Details of the calorimeter electronics design will be explained in later sections. Using 5 W per tower plus a 20% contingency, the total power budget for the full flight calorimeter is ~ 150 W, well within the 200 W allotted in the NRA.

Component	Power/unit (mW)	Quant.	Total (mW)
ASIC Channel	0.72	320	230
Preamplifier	0.13		
Shapers	0.025		
Peak Detect	0.035		
Discriminators	0.035		
DACs/Mltplx	0.30		
FPGA	40	40	1600
ADC	3	160	480
Clocks	150	4	600
DSP	1000	1	1000
Drivers/Misc			1000
TOTAL			4910

Table III-3. Calorimeter Power Budget for a Single Tower

The preliminary mass budget is heavily dominated by the CsI mass itself, which is well understood. The photodiode readouts, consisting of merely ~ 1 cm² of silicon, are nearly massless. Hence, there is very little uncertainty in the total mass of this calorimeter. No contingency is needed for the mass of the crystals themselves or the detectors. Table III-4 shows the detailed mass estimate for a single tower, including electronics. The full flight calorimeter, at 2,350 kg, fits within its assigned NRA mass budget.

The CsI calorimeter is an integral part of the proposed tower concept and is designed to the tower mechanical dimensions. As such, the calorimeter subsystem is ~ 33 cm \times 33 cm in frontal area and ~ 36 cm deep. A 5 \times 5 array of these would therefore fit within the allotted 1.7 \times 1.7 \times 0.4 m.

III.4 Current Status of Calorimeter R&D

Substantial progress has already been made in the design of the proposed calorimeter. Work has concentrated on four areas: (1) CsI and PIN diode detector module performance and packaging; (2) low-power analog front-end electronics and data acquisition electronics; (3) mechanical design and packaging of the calorimeter; and (4) science support and performance verification.

1. CsI and PIN diode detector module performance and packaging. To date, we have built two prototype calorimeters.

First prototype. The first prototype followed the baseline design proposed under the NASA New Mission Concept in Astrophysics study (Michelson et al. 1994) and had CsI crystals with their long axes perpendicular to the planes of silicon (i.e. gamma rays normally incident on the tracker planes would be parallel to the crystal axes). The position information for on-axis beams was limited by the crystal segmentation. This prototype consisted of a 5 \times 5 array of crystals, each 3 \times 3 \times 19 cm long. The crystals were read out with 1 \times 1 cm commercial PIN diodes at each end. The diodes were instrumented with laboratory hybrid preamplifiers and NIM and CAMAC shaping amplifiers, discriminators, and ADCs. The system was tested at a beam test at SLAC in the summer of 1996. During that beam test, some data were taken with the beam perpendicular to the long axis of the crystals, demonstrating the excellent positioning capabilities in the orthogonal dimension.

Second prototype. The second prototype consisted of an eight-layer hodoscopic array. The array recycled the crystals from the original prototype and added seven crystals to provide 32 live crystals in the stack. Again we used laboratory electronics. The calorimeter was operated in conjunction with a prototype tracker at a beam test at SLAC in the Fall of 1997. Various energy electron and photon beams were used to test the response to electromagnetic showers. The second prototype was also tested with hadronic beams

Component	Mass (kg)
CsI	77.2
Wrapping, Pads, etc	2.5
Mechanical	5.4
Electrical	5.0
PC boards	1.0
Components	1.0
Connectors	1.0
Controller	2.0
Margin	4.0
Total	94.1

Table III-4. Calorimeter Mass Budget for a Single Tower

(protons, Helium and Carbon) at the National Superconducting Cyclotron Lab (NSCL) at Michigan State University in January 1998. The results of the beam tests are shown later in this section.

Custom PIN diodes. The large dynamic range requirement on the energy coverage of individual crystals has led to a design with two PIN photodiodes of differing active areas at each end of the crystal. While in principle the ratio of areas of the two diodes could accommodate an arbitrarily large dynamic range, extreme caution must be exercised to ensure the smaller PIN diode is not affected by electronic or optical coupling to the larger diode. The current design therefore uses a ratio of areas of 4:1, with the remaining difference in dynamic range being accommodated in the amplifier circuitry. At the 1997 SLAC beam test we demonstrated the performance of the two-diode concept with standard, commercial PIN diodes ($\frac{1}{4}$ cm² and 1.0 cm² areas) in individual packages.

Radiation-hardness tests. We have exposed CsI crystals to increasing doses of gamma rays at NRL's ⁶⁰Co Irradiation Facility and intense beams of energetic protons at NSCL. The ⁶⁰Co tests show that after 20 kR (~20 years of exposure in the GLAST orbit), the light yield has decreased by ~25%. The crystal exposed to the hadron beam is still being studied. Further testing is planned (see Section III.5).

2. Low-power analog front-end electronics and data acquisition electronics. A prototype front-end Application Specific Integrated Circuit (ASIC) has been designed by NASA/GSFC and Prime Circuits Inc. It contains preamplifiers, shapers, discriminators, and peak-hold circuitry for both PIN diodes from one end of a CsI crystal. Each diode signal is first sent to a charge-sensitive preamplifier, then is amplified through two shaping amplifiers with differing gains to increase the overall dynamic range of the system (see Figure III-3). The shaped signal is put through a peak-hold circuit, which drives the output of the ASIC to an external Analog to Digital Converter (ADC) to digitize. The unique requirements of this application are the need for a relatively long shaping time, good linearity, and large dynamic range, while maintaining low

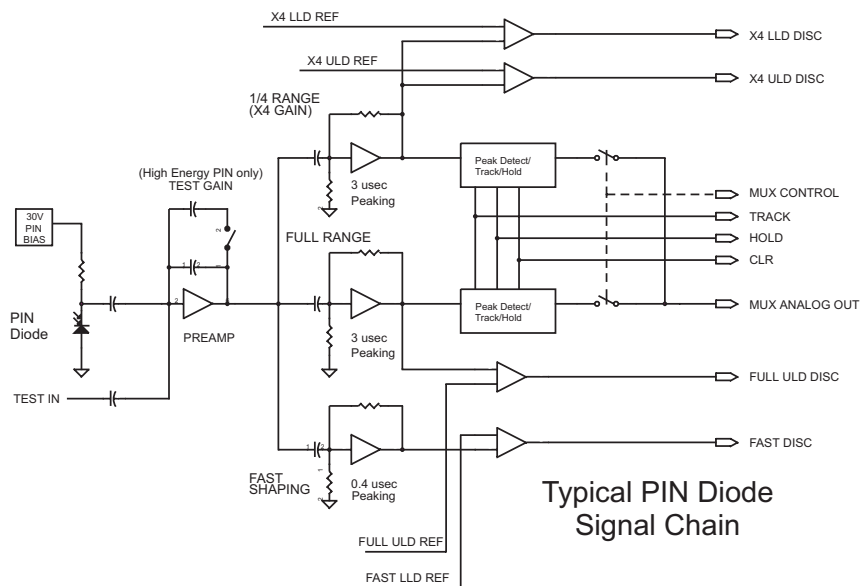


Figure III-3. CMOS Front-End Electronics Block Diagram

power consumption. The ASIC design has been submitted to a foundry, and the first ASICs will be available for testing at the end of March 1998.

3. Mechanical design and packaging. The current mechanical design was outlined in Section III.2. The design fulfills the requirements of holding ~100 kg of material against Delta II launch loads (roughly 10 g vertically and 3.5 g transversely) with minimal gaps in the calorimetry caused by the modularity. Less than 1 cm of lightweight, low-Z material provides the mechanical support at the sides of the tower. The design is additionally complicated by the requirements to accommodate the large coefficient of thermal expansion of the CsI and the need for access to the crystals on the side of each tower for the diode readouts and the circuitry to convey the signals down to the bottom of a tower. Preliminary modeling of the proposed structure indicates it will meet the load and stiffness requirements.

4. Science performance and verification. The principle goals for the calorimeter at the 1997 SLAC beam test included (1) mapping of the CsI crystal response, i.e. the light-collection efficiency, as a function of position for a number of crystal geometries and readouts; (2) measuring the position and angular resolution of the hodoscopic CsI array with electromagnetic showers; and (3) measuring the energy resolution as a function of incident energy, including a demonstration of shower-profile fitting.

Extensive Monte Carlo simulations of the hodoscopic calorimeter in a number of configurations have been performed at NRL and GSFC to predict performance at the beam test and in flight. The Monte Carlo studies have all utilized the GISMO package. GISMO is a library of C++ classes from which one can build applications that allow simulation of any CsI GLAST calorimeter design. Gamma ray induced electromagnetic showers are simulated in the calorimeter and the energy deposition per CsI log as well as the energy weighted position along the long axis of each log are recorded. This information is then used to reconstruct the direction of the incident gamma ray. Work is in progress determining the optimal crystal dimensions and algorithms for this reconstruction.

In Figure III-4 we show the results for photons of energies 1-10 GeV incident at 30 degrees with respect to the normal to the calorimeter face. In this figure we quote the 68% confinement radius of the angular deviations of the reconstructed directions from the true direction. This is shown for two different crystal dimensions. We have also calculated this quantity for other angles and do not find much variation within 60 degrees. The reconstruction algorithm used here is essentially the determination of the principle axis of the shower distribution with positions weighted by the energy deposited in each crystal. We have experimented with other algorithms and weighting schemes to optimize the angular reconstruction. We find that some algorithms can do better in certain angular ranges and crystal dimensions but induce systematic offsets for other parameter ranges. Determining which algorithm works best for a given angular range and crystal dimension is a major goal of future Monte Carlo studies.

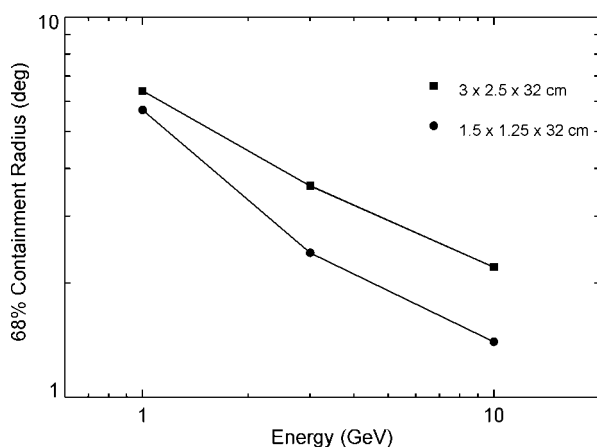


Figure III-4. Angular resolution vs energy for two CsI crystal sizes from simulations.

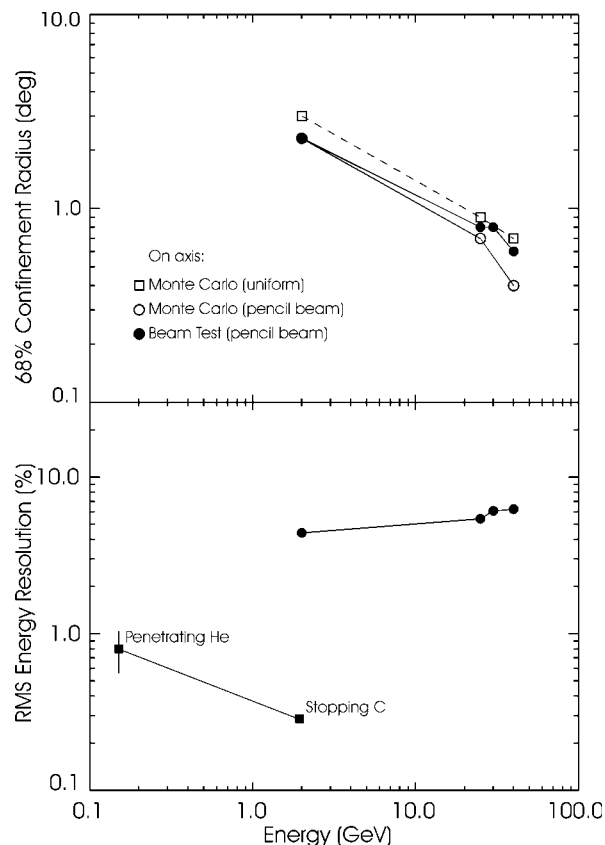


Figure III-5. Upper panel: Measured angular resolution for calorimeter-only events from SLAC beam test, compared with Monte Carlo predictions. Lower panel: Measured energy resolution of CsI array for electromagnetic showers and nuclei.

Energy reconstruction by shower profile fitting. The principle function of the calorimeter is to measure the energy of incident gamma rays. At the lower end of the sensitive range of GLAST, where electromagnetic showers are fully contained within the calorimeter, the best measurement of the incident gamma-ray energy is merely the sum of all the signals in the CsI. At energies above ~ 1 GeV, an appreciable portion of the shower escapes out the back of the calorimeter. Furthermore, as the incident energy increases, a decreasing fraction of that energy is deposited in the calorimeter, and *fluctuations* in the shower development create a substantial tail to low energy depositions as, e.g., some showers begin later in the calorimeter.

We employ two complementary methods of correcting the measured energy deposition. The first method, which is appropriate for spectral deconvolution of an ensemble of detected gamma rays, requires the creation of an instrument response matrix that transforms measured energy deposition to incident energy as a

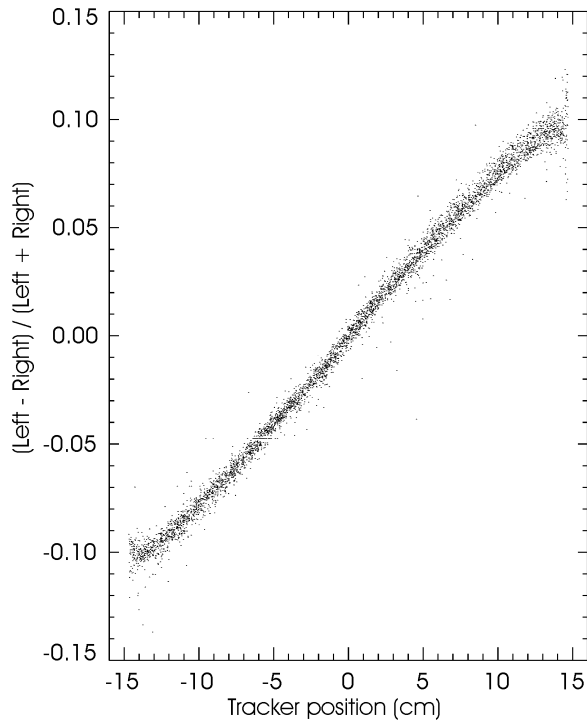


Figure III-6. Proportionality between asymmetry of light collection and position of interaction within CsI crystal.

function of zenith and azimuth angle. The columns of this response matrix are Green's functions, i.e. the spectra that should be produced by monoenergetic beams, at a large number of incident energies. A candidate incident spectrum is then multiplied by the response matrix and compared to the observed spectrum. Parameters of the candidate spectrum are varied to minimize χ^2 . Such forward-folding spectral deconvolution is standard in gamma-ray astronomy and is currently employed in EGRET data analysis.

The second method, shower profile fitting, is appropriate for reconstructing the energy of individual photons. The mean longitudinal shower profile is well-described by simple analytic functions, e.g. the gamma distribution of Grindhammer et al. (Proc. Workshop on Calorimetry for the Supercollider, Tuscaloosa, AL, ed. R. Donaldson and M.G.D. Gilchriese (World Scientific, Teaneck, NJ, 1989), p. 151), which is a function only of the location of the shower start and the incident energy. Because the calorimeter is longitudinally segmented, the observed energy deposition in each layer can be fit with this simple two-parameter model.

The lower panel of Figure III-5 shows the energy resolution achieved for electron beams of 2 GeV, 25 GeV, 30 GeV, and 40 GeV at the 1997 SLAC beam

test. With a measured resolution of $\sigma_E/E = 4\%-7\%$ for 2-40 GeV, the prototype hodoscopic CsI calorimeter clearly more than meets the requirements for GLAST specified in Table 2 of the NRA.

We emphasize also that the energy resolution above ~ 1 GeV is limited by the statistics of shower fluctuations in any calorimeter of this depth. The intrinsic energy resolution of the CsI calorimeter is quite good: tests we conducted at NSCL demonstrate $\sigma_E/E = 0.3\%$ at 2 GeV with a carbon beam (0.8% at 150 MeV with a helium beam), as indicated in the lower panel of Figure III-5.

Position reconstruction and imaging calorimeter. In addition to shower profile fitting, the segmentation of the CsI calorimeter allows spatial imaging of the shower and accurate reconstruction of the incident photon direction.

Each CsI crystal provides three spatial coordinates for the energy deposited in it, two coordinates from the physical location of the CsI bar in the array and one coordinate along the length of the bar from the difference in light level measured in the photodiode at each end. If the light falls off linearly with distance from the diode, then the position is exactly proportional to the difference in light levels at each end. Scaling the difference by the total signal removes the energy dependence from the proportionality. Thus the position is given by the "light asymmetry measure", $x = (\text{Left} - \text{Right}) / (\text{Left} + \text{Right})$.

Figure III-6 demonstrates that the light asymmetry is indeed simply proportional to the shower position over the majority of the length of a prototype 32-cm CsI bar. True positions were determined by the prototype Si tracker for 2 GeV electrons, which typically deposited ~ 150 MeV in the CsI. In the figure, each dot represents the measurements of a single event. The rms error in the position determined from light asymmetry is $\sigma_x = 0.28$ cm for these data.

The measured rms position error is summarized in the following two figures. Figure III-7 shows the position error from three crystals at increasing depth in the 6x8 test array at four beam energies, 2 GeV, 25 GeV, 30 GeV, and 40 GeV. The dashed line indicates that the error scales roughly as $1/\sqrt{E}$, as one would expect if the measurement error is dominated by photoelectron statistics. Also shown are the position errors deduced from imaging cosmic-ray muons in the array and from the He and C beams at NSCL; these points fall below the trends established by the electron showers because

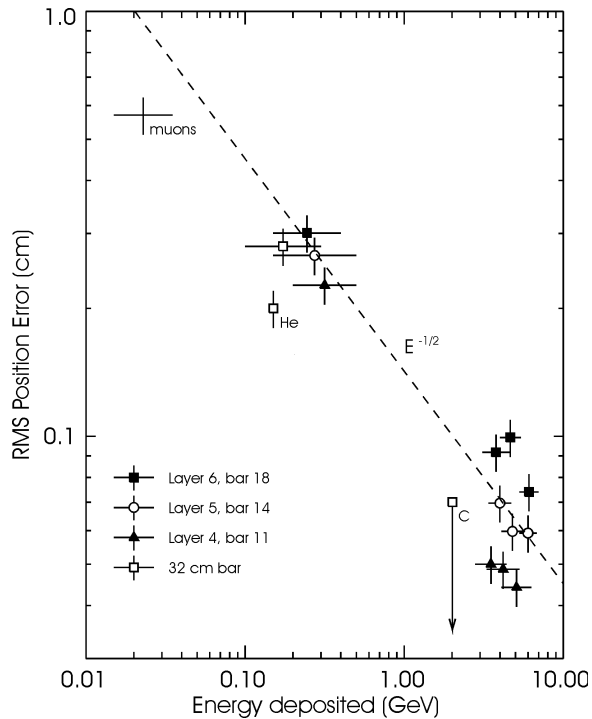


Figure III-7. Position resolution in CsI bars for EM showers, muons, He, and C.

ionization energy-loss tracks do not have the significant transverse spread that EM showers do.

The effect of the transverse shower development on position determination can be seen in Figure III-8. The rms position error is shown as a function of energy deposited and depth in the calorimeter (indicated by the ordinal layer numbers on the data points) for three beam energies. We see that position resolution is best early in the shower, where the radiating particles are few in number and tightly clustered physically, and at shower maximum, where the energy deposited is greatest and statistically easiest to centroid. The position resolution degrades past shower maximum, where the shower multiplicity falls and the energy deposition is spread over a larger area and varies from shower to shower.

To test the ability of the hodoscopic calorimeter to image showers, we reconstructed the arrival direction of the incident beam electrons from the measured positions of the shower centroids in each layer, without reference to the tracker information. The angular resolution, given by the 68% confinement space angle, is shown in the upper panel of Figure III-5, along with Monte Carlo predictions for a pencil beam (to simulate the accelerator test) and for uniform illumination on-axis. The beam test results *thus confirm the Monte Carlo predictions of 1-2 degree imaging performance* for calorimeter-only events at 10 GeV. Thus the hodoscopic calorimeter provides enhanced capability for pulsars, AGNs, and GRBs beyond that specified in the NRA.

Proposed Calorimeter Technology Development Program

III.5

Several advances in the supporting technologies and optimizations in state-of-the-art design and packaging of detectors for space missions are necessary before finalizing the design and constructing a full-scale prototype of a hodoscopic calorimeter module; however, we have already made substantial progress in developing this design as part of the GLAST SR&T program and the GLAST Mission Concept Study.

Because of the long lead times involved and the compressed timetable of the ATD program, we propose a

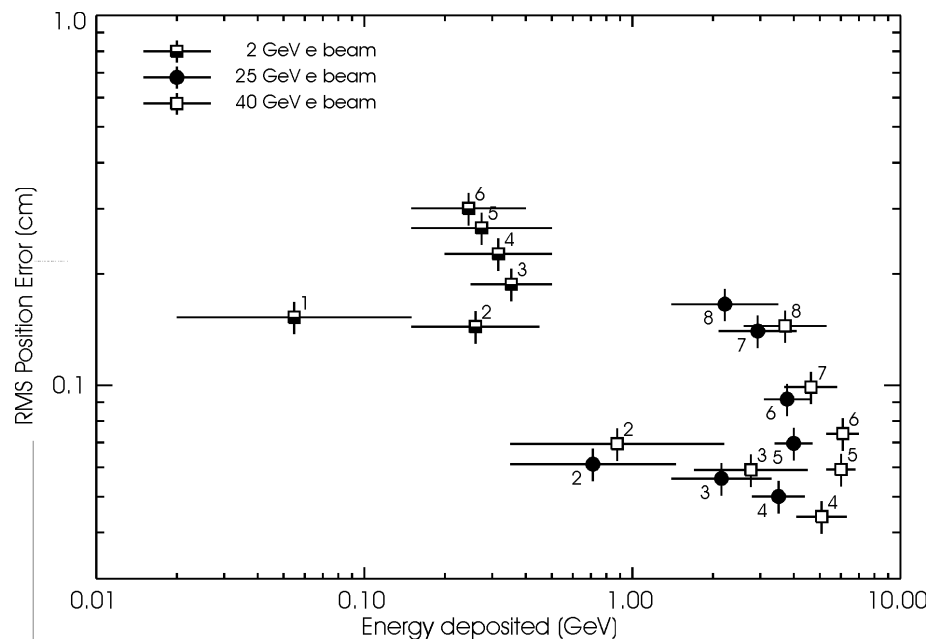


Figure III-8. Energy and depth dependence of position resolution. Ordinal numbers indicate layer in CsI stack.

dual track of building a prototype based on the lessons we have already learned and incorporating newer technologies as they become available during this ATD program. We discuss the technology development and prototype tower efforts separately below.

A. Technology Development

1. Science Performance Verification. Additional Monte Carlo simulations using the GISMO code will be performed at NRL and GSFC to optimize the angular and energy resolution of the calorimeter by varying the segmentation and spacing of the crystal array. For example, the beam test results indicate that halving the thickness of the first two layers of CsI would enhance shower imaging by improving the localization of the vertex of pair conversions within the calorimeter. Additional studies of background-rejection and particle recognition for calorimeter-only events will be performed using neural networks and rule-based algorithms.

2. CsI(Tl) and PIN photodiode detector module performance and packaging. The CsI crystals are essentially optical systems, the optical characteristics of which must be optimized to provide the best light collection (i.e. best signal to noise) as well as provide the differential light measurement between the ends of a crystal to permit determination of the position along the crystal at which the traversing particle created the light. These effects are controlled by the crystal surface preparation and polishing as well as by the reflective material and wrappings used to enhance the light transmission along the crystal.

The usual crystal surface treatments used in a laboratory environment are not necessarily applicable for GLAST because of the need to package the crystals to withstand launch loads and vacuum. The CsI is soft enough that the surface treatment could be affected by the pressure put on the crystals. To investigate these effects, we have constructed a pressure fixture in which wrapped crystals can be put under calibrated loads and subsequently inspected visually and with lab sources. The wrapping materials used in the laboratory might also not be ideal for space. For example, the best laboratory material (Tetrak) tends to trap pockets of air between the material and the crystal. We will investigate changing the properties of Tetrak with the manufacturer. Alternative wrapping materials such as Tyvek may suffer from the difficulty of creating a reproducible wrap. We will also investigate using various types of paint treatments as a substitute. Preliminary tests show this method might be more re-

producible and subject to better quality control than the wrapping techniques.

CsI crystals are known to suffer only modest degradation from radiation damage, with some evidence for a decrease in the attenuation length with increasing dose. Because a change in the attenuation length could be noticeable in the high aspect ratio GLAST crystals, we have begun a series of radiation damage tests (see Section III.4). These tests will continue under the ATD program. Radiation damage is documented to be dependent on the manufacturing process; thus we will test material from various batches of various vendors.

The response of PIN photodiodes to the thermal cycling, radiation and vacuum aspects of the space environment will be tested. To achieve the large dynamic range identified in Table III-5, the crystals will need a custom dual PIN diode design, one PIN for the low-gain electronics channel and the other for the high-gain channel. Care must be taken in the dual PIN design to avoid cross-talk between the two channels that can affect the overall system signal-to-noise performance. We are working with the manufacturer to design a custom dual PIN diode that simultaneously minimizes cross-talk and the total area and mass of the package, and has low-profile connectors as required to minimize dead space within the calorimeter.

3. Low-power, analog and data acquisition electronics. The prototype calorimeter ASIC (CSICAL-1) developed by NASA/GSFC and Prime Circuits Inc. will be the starting point for this effort. The ASIC will be tested in Spring 1998 with actual CsI-PIN diode signals and the noise and dynamic range performance measured. We expect this to lead to a second generation ASIC where the energy ranges and number of shaping channels per PIN are matched to cover the entire dynamic range required. A second generation ASIC will be required to add the control DACs and other peripherals not included in the first prototype.

The calorimeter data acquisition electronics concept is shown in Figure III-9. A FPGA (Field Programmable Gate Array) will be used to control up to eight individual ASICs. The FPGA will control the various DACs used to set up the ASIC, control the range to determine which signal goes to the ADC, control the ADC itself, control the relative timing between the ASIC and the ADC, read out the ADC, and act as a buffer between the ADC and the downstream DSP (Digital Signal Processor). The FPGA will also be the first level of electronics in the trigger logic to provide calorimeter-only triggers for high-energy events.

Parameter	Design
Number of channels	320/module
Dynamic range	$\sim 3 \times 10^5$
Noise goal	0.1 MeV ($10^3 e^-$)
A to D range	0.3 MeV - 100 GeV
Electronic resolution	$\sim 1\%$ (except at threshold)
Trigger rate (GLAST)	400 Hz (orbit avg.) 1.2 kHz (peak) 100 kHz (design max.)
Calorimeter-only trigger	> 1 GeV in any Crystal
Self-trigger delay	< 1 μ sec
Trigger dead time	< 10 μ sec
Power	5 W/module; <15 mW/chan (4 ch/xtal)

Table III-5. Calorimeter Readout Electronics Requirements

Fast space-qualified multiplexers and ADCs are needed to present the data to the GLAST data acquisition system within the specified processing time. The current plan is to use COTS (Commercial Off The Shelf) ADCs. Three commercial ADCs have been identified that meet the speed, accuracy, and power constraints required for the calorimeter. We will investigate whether these ADCs can be space qualified or what modifications would be required to make them qualifiable. Table III-5 is a summary of the readout

electronics requirements for the hodoscopic calorimeter configuration.

4. Mechanical design and packaging of the calorimeter. The current design of the calorimeter compression cell will be refined. The goals are to further reduce the dead space between compression cells and minimize the amount of dead material. The design will pay particular attention to the choice of materials and will maximize the use of low-Z materials. A Finite Element Model (FEM) will be prepared to assess the structural dynamic response, in particular to transverse acceleration. The finite element analysis will include a study of thermal strains induced by the wide environmental temperature variations anticipated for both terrestrial and space conditions. The calorimeter mechanical design will be integrated with the tracker design to develop a corner fixture that satisfies the stiffness requirements for both the CsI calorimeter and the silicon tracker; and to determine the CsI crystal temperatures as influenced by the tracker heat transport down the calorimeter sides.

B. Prototype Tower Development

A prototype hodoscopic calorimeter will be constructed under this NRA for mechanical, electrical, and science-verification testing. The prototype will be constructed during the Basic and Option 1 phases of the program and will test the key technology readiness in the following areas:

- The prototype will include the baseline mechanical design concept which minimizes passive material and supports expected thermal and launch en-

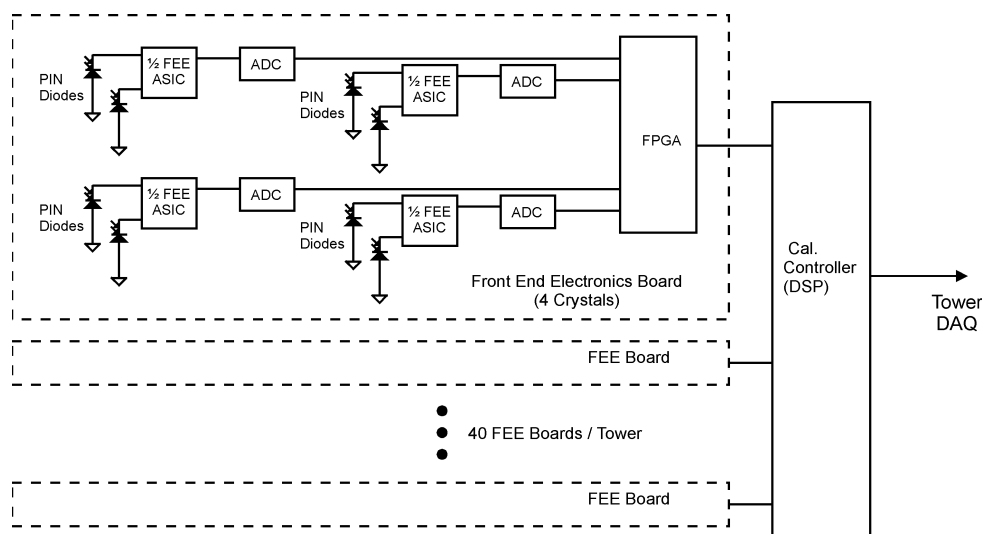


Figure III-9. Conceptual block diagram of the calorimeter readout electronics.

vironments. Energy resolution of the resultant configuration will be measured with muons and in accelerator beam tests.

- The prototype will include low-power front end electronics which achieve the required power budget and provide the required performance over the large dynamic range. Cosmic ray muons and accelerator beam tests measurements will verify performance.
- Angular resolution of the calorimeter will be measured in the prototype tower tests in conjunction with the tracker.

During the Basic and Option 1 phases of the program, the calorimeter development efforts are focused on 1) the optimization and fabrication of the detector elements and compression cell that holds them, and 2) the design and fabrication of the analog front end electronics which mount on the sides of the calorimeter. The completion of the calorimeter tower controller is delayed to the Option 2 phase of the program. Laboratory VME interface shall perform the functions of the calorimeter controller for the demonstration prototype testing. This organization has been selected due to funding constraints and the low risk associated with this component of the calorimeter subsystem. The complete calorimeter, including controller, will be available for the balloon flight scheduled in the Option 2 phase.

The fabrication of the prototype calorimeter begins with the base phase of the proposed program. This is required due to the long lead times required for the CsI crystals and PIN diodes. The previous two years of study of these calorimeter concepts and the two beam tests at SLAC in 1996 and 1997 have resulted in a mature baseline. We are continuing analysis of optimization studies for differing segmentations of the calorimeter but believe the baseline will demonstrate all critical technical issues. The optimization is balancing scientific performance against channel count (the number of segments) and associated mechanical and power requirements. These optimization studies will extend into Option 2 phase of the program.

III.6

Management and Organization of Calorimeter Development

Collaborating institutions on the calorimeter development are the Naval Research Lab (NRL) and Goddard Space Flight Center (GSFC). The calorimeter subsystem development manager is Dr. W. Neil Johnson, Naval Research Lab. He directly oversees all aspects

of the calorimeter development. Because of the critical mechanical interfaces between the tracker and the calorimeter, close coordination of the mechanical engineering tasks will be managed by Bruce Feerick (SLAC) who is responsible for overall tower integration. Table III-6 shows the organization of the calorimeter efforts and the responsibilities of the collaborators.

The calorimeter electronics efforts are the joint responsibility of NRL and GSFC. GSFC is responsible for the design of the analog front end application specific integrated circuits (ASICs). NRL is responsible for the overall electronics architecture, design, fabrication, integration and test.

During the testing phase, the calorimeter is integrated into the GLAST prototype tower under the leadership of Stanford University and SLAC. The prototype tower accelerator beam test will be directed by SLAC and American University.

Dr. Jay Norris, GSFC, is responsible for performance and science optimization simulations.

WBS	Task	Institutions
3.1	Management	NRL
3.2	CsI Detector Module	NRL
3.3	Analog Front End Electronics	NRL, GSFC
3.4	Compression Cell	NRL
3.5	Calorimeter Tower Controller	NRL
3.6	Assembly	NRL
3.7	Test & Calibration	NRL
3.8	Design & Verification	
3.8.1	Design/Simulations	GSFC NRL
3.8.2 - 4	Design/Verification	NRL
3.8.5	Balloon Flight	NRL GSFC

Table III-6. Calorimeter Development WBS and Responsibilities

III.7 Schedule for Calorimeter Development & Demonstration

Table III-8 summarizes the calorimeter technology program as it pertains to the demonstration prototype tower. An outline of the program was presented in Section III.5.B, Prototype Tower Development.

III.8 Small Business & Small Disadvantaged Business Subcontracting Plan

NASA’s socio-economic goals for SB/SDB Subcontracting are understood and supported. The Naval Research Lab’s SB/SDB goals are developed in accordance with DoD directives. In FY97, NRL’s SB goal was 55.0% and it exceeded this goal, achieving 56.9%. The SDB goal in FY97 was 7.5%. Actual performance on the SDB objective was 6.24%. NRL has active contracts with multiple SB/SDBs that are to be used in the GLAST calorimeter development program.

Item	Potential Source
Machining and Assembly Services	Multiple SB/SDB
Project support	SB, Praxis, Inc.
Mechanical & Thermal Design/Support	SB, Swales & Assoc.
Electrical Design/Fab	SB, Silver Engineering
GSE & ADPE	Multiple SB/SDB
GSE & Subsystem Software	SB, Software Technology, Inc.

Table III-7. SB/SDB Industry Categories

Examples of industry categories and potential sources are indicated in Table III-7.

Date	Item	Milestone
6/01/98	Start Program	First prototype FEE ASIC already tested
6/01/98	Submit second FEE ASIC	
6/01/98	Order first prototype custom PIN diode	Custom PIN diode already designed
7/01/98	Order CsI crystals	Crystal design frozen
7/01/98	Start design of FEE board and FPGA interface	
8/01/98	Start final design of compression cell	Inner and outer volume of comp. cell defined
9/01/98	Start test of second prototype FEE ASIC	Second prototype ASIC delivered
9/15/98	Test of first prototype PIN diode	Delivery of first custom PIN diode
10/01/98	Start crystal acceptance testing	First crystal delivery
11/01/98	Submit Flight version of FEE ASIC	FEE ASIC design frozen
11/15/98	Order batch of (modified)PIN diodes	Design of custom PIN diode frozen
12/01/98	Order lab DAQ modules	ICD for beam test DAQ frozen
12/15/98	Start compression cell fabrication drawings	Compression cell design frozen
1/15/99	Send compression cell to fabrication	
1/15/99	Order boards and parts for FEE readout	FEE board design frozen
2/01/99	Test flight version of FEE ASIC	Flight version of FEE ASIC delivered
2/15/99	Acceptance of last crystal	Last crystal delivered
2/15/99	Start assembly of detectors	Custom PIN delivered
3/01/99	Start assembly of FEE boards	
4/01/99	Start assembly of detector stack	Compression cell delivered Last detector tested
4/15/99	Test lab/beam test DAQ	All lab/beam test DAQ hardware delivered
5/01/99	Start assembly of FEE boards on comp. cell	FEE boards assembled and tested
6/15/99	Start testing calorimeter with lab. DAQ	Prototype Calorimeter complete
7/15/99	Start calibrations	Calorimeter working and debugged
8/01/99	Ship calorimeter for integration in Tower	Calorimeter tests complete
8/15/99	GLAST Tower Prototype assembly complete	GLAST Tower Prototype cosmic ray test begins
9/01/99	GLAST Tower Prototype beam test begins	Validation of GLAST Tower Prototype
1/01/00	Calorimeter DAQ board sent out	Design of calorimeter DAQ frozen
4/30/00	Construction and test of DAQ completed	
5/31/00	Integration of DAQ completed	Full engineering prototype built
7/31/00	Test of calorimeter with own DAQ complete	Full engineering prototype tested
9/01/00	Balloon flight of Tower Prototype	Full engineering prototype flown
12/15/00	Science Measurement System Final Report	

Table III-8. Schedule Milestones for the GLAST Calorimeter Prototype